


# RNA-seq identifies differentially expressed genes involved in *csal1* overexpression in granulosa cells of prehierarchical follicles in Chinese Dagu hens

Hongyan Zhu,\* Yi Ding,\* Jianglan Zhu,\* Lingjun Zhao,† Yuhong Su,‡ and Song Zhao <sup>§,1</sup>

\*College of Basic Medical Science, Jinzhou Medical University, Jinzhou 121001, Liaoning, China; †College of Animal Husbandry and Veterinary, Jinzhou Medical University, Jinzhou 121001, Liaoning, China; ‡College of Food and Health, Jinzhou Medical University, Jinzhou 121001, Liaoning, China; and §College of Life Science Institute, Jinzhou Medical University, Jinzhou 121001, Liaoning, China

**ABSTRACT** The transcription factor *csal1* is an important molecule that plays a critical regulatory function in ovarian follicle development, as confirmed by our previous data. However, the candidate genes of *csal1* and its regulatory mechanism remain poorly understood in the granulosa cells (GCs) of chicken prehierarchical follicles (PFs). Six transcriptomes of *csal1* and empty vector were analyzed in Chinese Dagu hens by RNA sequencing. Six cDNA libraries were constructed, with more than 42 million clean reads and 16,779 unigenes. Of these 16,779 unigenes, 2,762 differentially expressed genes (DEGs) were found in GCs, including 1,605 upregulated and 1,157 downregulated unigenes. Fourteen genes, including *BMP5*, *TACR2*, *AMH*, *PLAG1*, *MYOD1*, *BOP1*, *SIPA1*, *NOTCH1*, *BCL2L1*, *SOX9*,

*ADGRA2*, *WNT5A*, *SLC7A11*, and *GATAD2B*, were related to GC proliferation and differentiation, hormone production, ovarian follicular development, regulation of reproductive processes, and signaling pathways in the PFs. Further analysis demonstrated the DEGs in GCs of ovarian follicles were enriched in neuroactive ligand–receptor interaction, cell adhesion molecules, and pathways related to cytochrome P450, indicating a critical function for *csal1* in the generation of egg-laying features by controlling ovarian follicle development. For the first time, the current study represents the transcriptome analysis with ectopic *csal1* expression. These findings provide significant evidence for investigating the molecular mechanism by which *csal1* controls PF development in the hen ovary.

**Key words:** Chinese Dagu hens, *csal1*, differentially expressed gene, ovarian follicle, transcriptomics

2023 Poultry Science 102:102310

<https://doi.org/10.1016/j.psj.2022.102310>

## INTRODUCTION

Ovarian follicle development in hens represents a greatly complex event that involves multiple endocrine, paracrine, and autocrine processes spatially and temporally. It features substantial alterations in the course of follicle selection (Woodruff and Shea, 2007). The problem of follicular development can result in reduced reproductivity, especially low egg-laying rates, which constitute a major economic feature in poultry industry worldwide. A strict control of follicular hierarchy occurs in hens (Chen et al., 2021). Only a single dominant follicle is usually recruited into the preovulatory hierarchy in approximately one day, which is selected from 6 to 8-mm diameter prehierarchical

follicles (PFs), reaches maturity, and undergoes ovulation. Therefore, PF development is very important. Diverse biological processes, cellular components, molecular functions, or some signaling pathways may affect proliferation, differentiation, hormone production, secretion of granulosa, regulation of reproductive processes, and even growth in PFs (Xu et al., 2018). In the ovary, granulosa cells (GCs) constitute a critical site of estrogen biosynthesis for local utilization and provide endocrine signals to other tissues (Nelson and Bulun, 2001).

In recent years, RNA sequencing (RNA-seq) has been instrumental in functional genomics. The information about all the transcripts of an organism in a particular state could be generated in a comprehensive and quick manner to solve complex biological problems (Miao et al., 2016; Wu et al., 2020; Wang et al., 2021b). Several studies also revealed many mRNA transcripts in ovarian follicles (Yang et al., 2008; Wang and Ma, 2019), which are associated with genetic improvement in the domestic chicken breed.

© 2022 The Authors. Published by Elsevier Inc. on behalf of Poultry Science Association Inc. This is an open access article under the CC BY-NC-ND license (<http://creativecommons.org/licenses/by-nc-nd/4.0/>).

Received July 27, 2022.

Accepted October 31, 2022.

<sup>1</sup>Corresponding author: [zhaosong517@163.com](mailto:zhaosong517@163.com)

Chinese Dagu chicken is an important animal resource, which has been bred for more than 200 yr. It is widely distributed in Liaoning Province of China, mainly produced in Zhuanghe City of Liaoning Province, so it is also called Zhuanghe chicken. Chinese Dagu chicken is a dual-purpose local chicken breed characterized by large eggs. The chicken is large and solid, with strong foraging ability, quality and quantity eggs, thick and solid eggshell, fresh and tender meat, and strong disease resistance. Our study had confirmed the correlation between *csal1* and laying traits of Chinese Dagu chicken (Zhu et al., 2018). However, the commercial production of Chinese Dagu chicken lacks systematic research on their laying performance. So, RNA-seq was carried out for identifying DEGs between overexpression and normal expression of *csal1* in GCs of hen ovarian prehierarchal follicles to comprehensively characterize the regulatory role of *csal1* in PF development.

Chick orthologue of the SALL1 gene, *csal1*, is a member of chicken spalt family which was characterized by multiple C2H2-type zinc-finger motifs (ZFs). To date, three members of the spalt family have been identified including *csal1*, *csal3*, and *csal4*. As a transcriptional repressor, the expression of *csal1* is predominantly detected in the developing heart, mesoderm, ectoderm, and neural tube of the early embryo (Sweetman et al., 2005). Our previous study, which was the first related report, showed that *csal1* suppresses the GC proliferation and steroidogenesis to regulate development and growth of ovarian follicles (Zhu et al., 2019).

Here, we aimed to obtain downstream target genes of *csal1* in GCs from PFs through high-throughput transcriptome technology, which were the key candidate genes contributing to ovarian function control, thus influencing egg-laying potential. The study also focused on the regulatory role of *csal1* in the biological processes and pathways associated with egg-laying in Chinese Dagu chicken. Additionally, RNA-seq data were validated by quantitative real-time polymerase chain reaction (RT-qPCR). This study provided important evidence for exploring the mechanisms underpinning egg-laying in poultry, and then provide molecular genetic markers for better egg production in the indigenous Chinese chicken breeding.

## MATERIALS AND METHODS

### Chicken and Samples

Chinese Dagu hens, provided by the Farm of Jinzhou Medical University, were euthanized at the age of 21 wk ( $n = 10$ ), and their PFs (6 to 8-mm diameter) (Gilbert et al., 1983) were collected for experiments. GCs from PFs (6 to 8-mm diameter) underwent culture as reported in a previous study (Zhu et al., 2019). All the procedures involving animals followed the guidelines formulated by the Ministry of Agriculture of the People's Republic of China, with approval from the ethics committee of Jinzhou Medical University (201805024, Jinzhou, China).

### Cell Culture and Cell Transfection

GCs were obtained as described in our previous report (Zhu et al., 2019). The specificity of GCs was detected by fluorescent and H&E staining procedures (Lyu et al., 2016). Simply, the pYr-adshuttle-4-*csal1* plasmid and the corresponding empty vector were transfected into GCs with Lipofectamine 2000 (Invitrogen, Carlsbad, CA). The generation of pYr-adshuttle-4-*csal1* has been described previously (Zhu et al., 2019). Cells ( $10^5$ /well in 24-well plates) were cultured in basal medium with 1  $\mu$ L/mL polybrene (Sigma, St. Louis, MO) at 37°C in a humid environment containing 5% CO<sub>2</sub> (Xu et al., 2018) for 24 h.

### Library Construction and Illumina Sequencing

Total RNA extraction utilized TRIzol Reagent (Invitrogen). RNA purity and amounts were assessed on a NanoDrop 8000 (Thermo Fisher Scientific, Waltham, MA) and a Bioanalyzer 2100 system (Agilent, Santa Clara, CA). RNA (3  $\mu$ g) was utilized for RNA-seq. The remaining RNA was kept at -80°C for validation assays. cDNA library construction utilized TruSeq RNA Sample Preparation Kit (Illumina, San Diego, CA), as directed by the manufacturer. The mRNA purification from total RNA utilized poly-T oligo-linked magnetic beads. 300-bp cDNA fragments were screened, AMPure XP system (Beckman Coulter, Fullerton, CA) was used for library fragment purification. DNA fragments containing adaptors at both ends underwent selective enrichment with the Illumina PCR Primer Cocktail by PCR amplification (15 cycles). Finally, PCR products underwent purification (AMPure XP system), and the quality of libraries was evaluated on a Bioanalyzer 2100 system.

### RNA-Seq Data Analysis

The prepared libraries underwent sequencing by next-generation sequencing on Illumina HiSeq 2500. Raw reads (FASTQ format) were refined by removing low-quality reads as well as adaptors with in-house perl scripts to yield clean reads. Meanwhile, the contents of Q20, Q30, and N (fuzzy base) in raw data were determined. Clean reads were used in all downstream analyses, with alignment with the reference genome carried out with HISAT 2.1.0 (Pertea et al., 2016; Kim et al., 2019).

The reads mapped to various genes were separately counted using the HTSeq v0.6.1 software (<https://htseq.readthedocs.io/en/master/>). Gene expression levels were reflected by the amounts of fragments per kilobase of transcript per million fragments (FPKM) after normalization. The expression patterns of DEGs were assessed with the Multi-Experiment Viewer software v4.9.0 (<https://mybioinformatics.com/mev-4-6-2-multiple-experiment-viewer.html>) according to the normalized FPKM + 1 value between the case and control groups after normalization. The Benjamini and Hochberg's

method was utilized to control the false discovery rate and derive the adjusted  $P$  value ( $P_{adj}$ ). The degree of gene expression was expressed as  $|\log_2\text{FoldChange}|$  ( $\text{Log}_2\text{FC}$ ). Genes with  $P_{adj} < 0.05$  and  $\text{Log}_2\text{FC} > 1$  were identified with DESeq. Volcano plots for visualizing significantly regulated genes were obtained with the R package “ggplot2” (v3.5.0) (Wang et al., 2010). The R program was utilized for data analysis, including principle component analysis (PCA).

## Gene Ontology and Kyoto Encyclopedia of Genes and Genomes Analyses of DEGs

Gene Ontology (GO; <http://www.geneontology.org/>) enrichment analysis was used for annotating and analyzing DEGs (Ashburner et al., 2000). GO terms include cell component (CC), molecular function (MF) and biological process (BP), in which DEGs were enriched. Bonferroni corrected  $P < 0.05$  was used as a criterion for GO annotation. Kyoto Encyclopedia of Genes and Genomes (KEGG; <http://www.genome.jp/kegg/>) was used to assess pathway enrichment. KEGG is a comprehensive database resource for analyzing DEGs through KEGG pathway enrichment. The results with  $P < 0.05$  and an FDR close to 0 were considered significantly enriched by DEGs.

## Protein Interaction Analysis

DEG–protein interactions were analyzed with STRING (<http://string-db.org/>). DEG–protein

interaction network data files were visually edited using Cytoscape v3.5.1 (<http://www.cytoscape.org/>).

## RNA-Seq Validation by RT-qPCR

Fourteen candidate genes were screened to validate RNA-seq data by RT-qPCR. Total RNA was isolated from *csal1*-transfected cells at  $1 \times 10^6$ /well using an RNA extraction kit (TaKaRa, China), and the first strand cDNA was synthesized from 1  $\mu\text{g}$  of total RNA using PrimeScript RT reagent Kit (TaKaRa, RR047A) according to the manufacturer’s instructions. *Csal1* and *18S rRNA* amounts were examined by RT-qPCR with TB Green (TaKaRa, RR820A) on a 7500 Fast Real-Time PCR System (Applied Biosystems, Grand Island, NY). The  $2^{-\Delta\Delta C_t}$  method was used for determining relative mRNA amounts, normalized to 18S rRNA expression. Table 1 showed all RT-qPCR primers (TaKaRa). Three independent triplicate assays were carried out.

## RESULTS

### RNA-Seq Data Quality

Six cDNA libraries were constructed for *csal1* overexpressing and control GCs from 6 to 8-mm diameter PFs using the Illumina HiSeq 2500 platform. RNA-seq raw sequences in each library ranged from 45,486,652 to 52,635,202 reads. Of these raw reads, >97.26% and 92.73% showed quality scores at the Q20 and Q30 levels, respectively. The highest N (base) frequency in raw data

**Table 1.** The sequences of genes for RT-qPCR.

Gene	Primer	Sequence (5'-3')	PCR products
18S	Forward	TAGTTGGTGGAGCGATTTGTCT	169bp
	Reverse	CGGACATCTAAGGGCATCACA	
<i>csal1</i>	Forward	CCCAGGAAGCAAGGTGTA	167bp
	Reverse	CGTTGGCATGTCCGTATT	
BMP5	Forward	GTGAGCAAAAGCAAGCAT	260bp
	Reverse	ATCAAAGTAGAGCACGGAG	
TACR2	Forward	CAGATTTGCTGATGTCCG	310bp
	Reverse	CACTTTGTGTCCCGTTG	
AMH	Forward	GGAGGAGATGGGACTTGGAG	261bp
	Reverse	AAGGCACTTTCATAGCGGG	
PLAG1	Forward	ATGATGGGTCTGGGGAGGT	311bp
	Reverse	TCGTGGTAGGGTGGTGGTT	
SLC7A11	Forward	GAAAAAACATACCCCTCG	214bp
	Reverse	CACCATTTCATAGACCCAAA	
MYOD1	Forward	CACGGGAACCCACAGGAGGA	352bp
	Reverse	AGCGAGGGCTGGAGGCATCT	
BOP1	Forward	CAGAGGAAGATGAGGGTGAACG	173bp
	Reverse	TCGGAGCCTGATGCCAAC	
SIPA1	Forward	GCCTCGGCTACATCCCCAAT	168bp
	Reverse	GACCCACCGTCTTCA	
NOTCH1	Forward	CTGGGGACACCACCTACGA	195bp
	Reverse	GCTGGCACTCATCCACATC	
BCL2L1	Forward	CTTTCAGCGACCTCACCTCC	192bp
	Reverse	ACACAATGCGTCCCACCA	
SOX9	Forward	AATACCTGCCCCCAACG	382bp
	Reverse	TACTGCGAGCGGGTGATG	
ADGRA2	Forward	TACACCAACGACATCACCCG	146bp
	Reverse	GCCACATAGAGGACATCAACCA	
WNT5A	Forward	CTTCAACGCACCCACCAT	151bp
	Reverse	GCAGCACATCAGTTCACAGC	
GATAD2B	Forward	GCTGGTGCTGCTGAAGAAG	105bp
	Reverse	GGAGATGGCTGGACGATAGA	

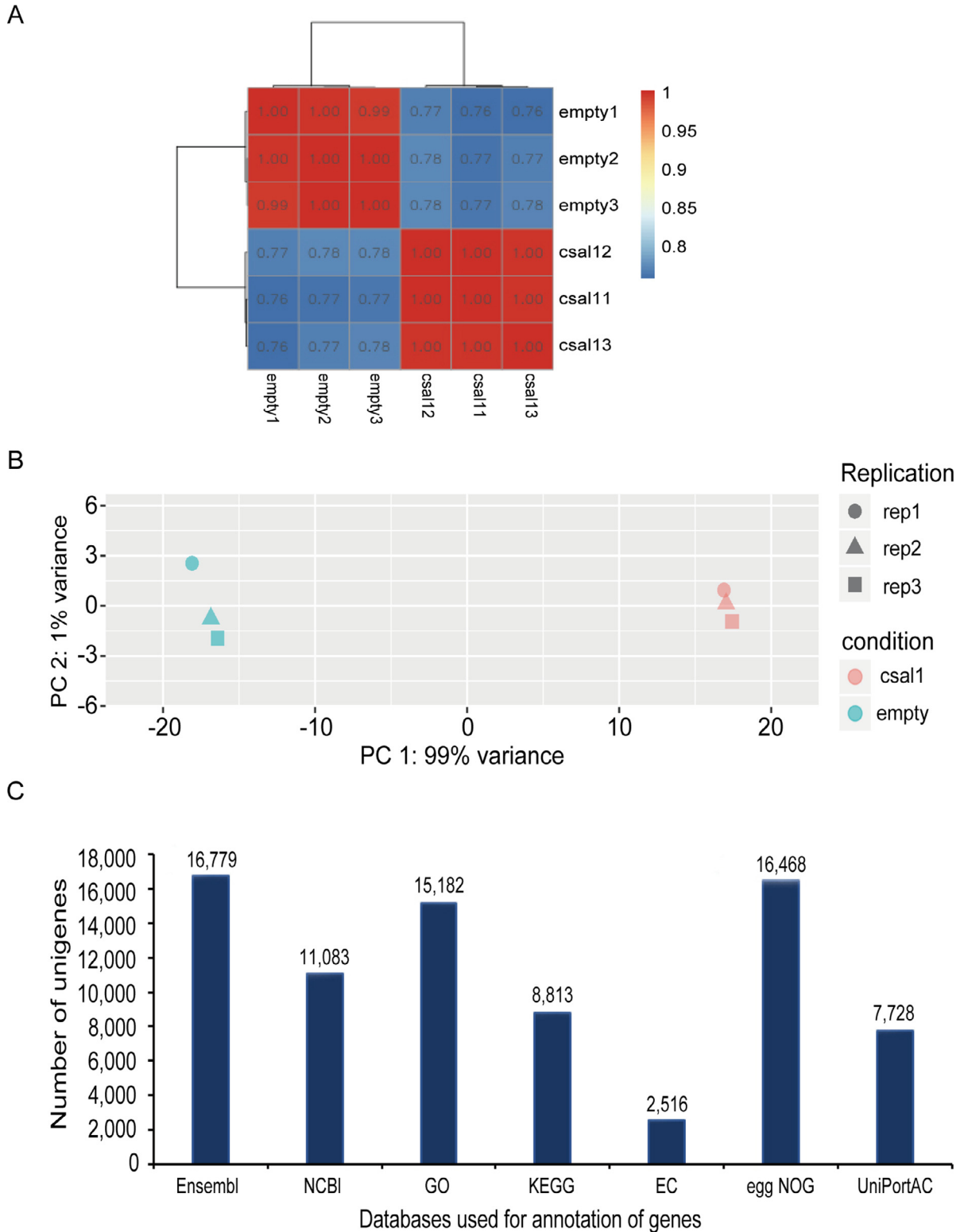


**Figure 1.** Features of sequencing data. (A) Pairwise Pearson's correlation analysis of sequencing data in triplicate for 2 specimens. (B) Principal component analysis (PCA) of transcriptomic variations. Shapes, distinct replication patterns of the collected cells; colored dots, distinct specimens. (C) Annotations of gene numbers according to various databases.

was 0.001% (Supplementary Table 1). After filtering, >41 million clean reads per library were obtained. High-quality clean reads and bases (bp) of clean data were 90.93 to 92.98% of all sequences of raw reads (Supplementary Table 2). The percentage of all mapped sequences/reads ranged from 92.43 to 94.17% of the clean reads. Mapped reads included 5.29 to 5.70% of clean

reads that were multiple mapped reads, and 94.30 to 94.71% of clean reads were uniquely mapped reads (**URs**) (Supplementary Table 3). Of all RNA-seq mapped events, read distribution was determined. All reads mapped to genes (**MGs**) covered 85.51 to 86.68% of the identified URs, and exons accounted for 73.67 to 89.03% of reads from MGs (Supplementary Table 4).

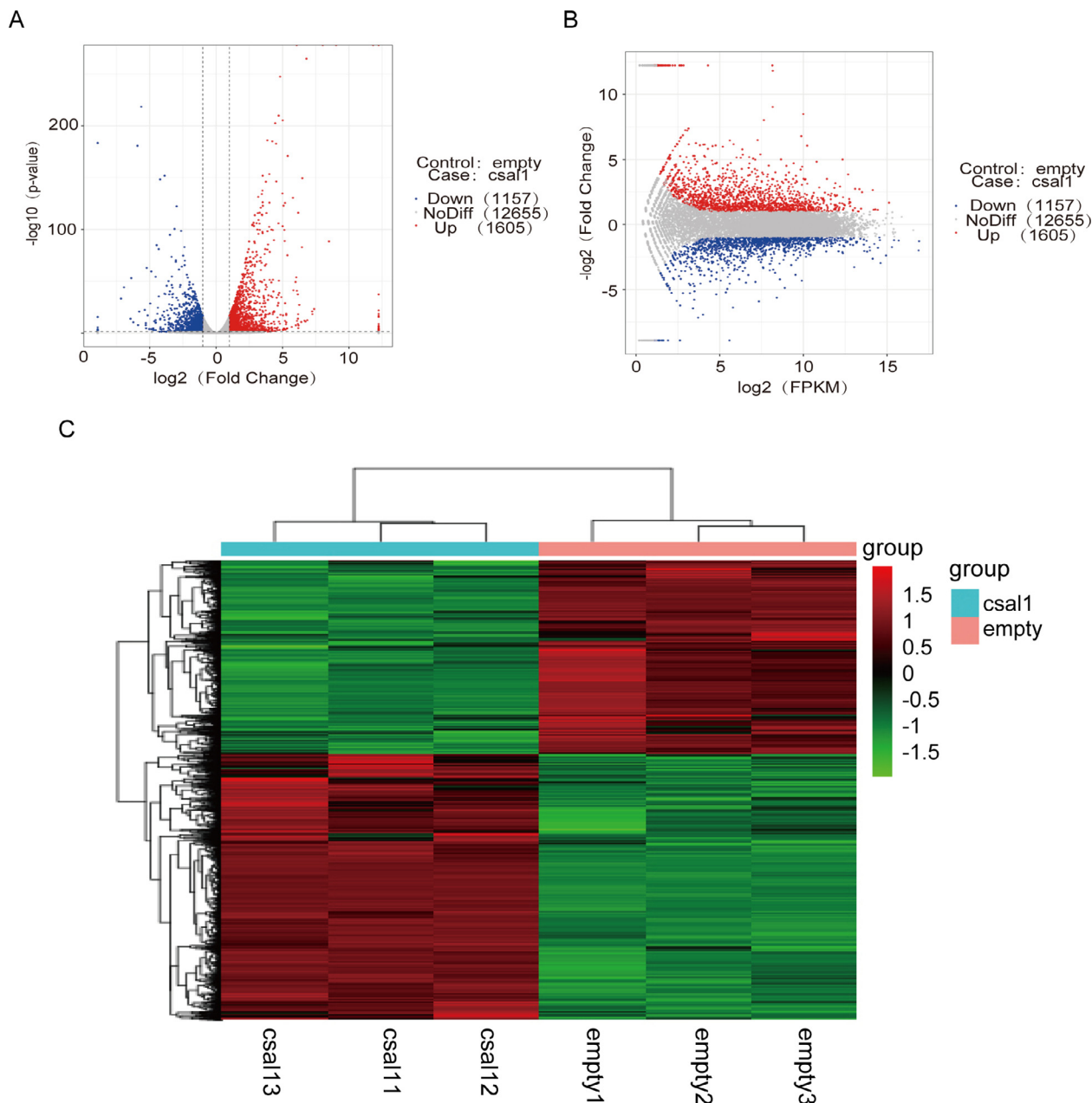


**Figure 2.** Detection and analysis of DEGs between *csal1* overexpressing and nontransfected granulosa cells from hen ovarian prehierarchal follicles. (A) Volcano plot of DEGs. The X-axis is  $\log_2$ foldchange; the Y-axis is  $-\log_{10}(P\text{-value})$ . The two vertical dashed lines show the two-fold change threshold; the horizontal dashed line shows a  $P_{\text{value}}$  of 0.05. Red, blue, and gray indicate significantly upregulated, downregulated, and non-differentially expressed genes, respectively. (B) MA of DEGs. The X-axis is  $\log_2$  Fragments per Kilobase of transcript per Million mapped reads (FPKM); the Y-axis is  $\log_2$ foldchange. Red, blue and gray dots represent significantly upregulated, downregulated, and non-differentially expressed genes, respectively. (C) Clustering of DEGs. Genes and samples are placed horizontally and as column, respectively. Red and green indicate high- and low-expression genes, respectively.

FPKM were quantified to assess gene expression, and Pearson's correlation coefficients of paired specimens with their biological replicates were  $>0.99$ , suggesting the general reproducibility of sequencing data, which was close to 0.8 (Figure 1A, Supplementary Figure 1). The values of PC1 and PC2 were, respectively, 99% and 1% from the PCA, and an overview of transcriptomic variation was obtained (Figure 1B). Genes with greatest variance (PC1) were further examined by GO analysis. The fastq files have been submitted to Sequence Read Archive database (SRA accession PRJNA854338).

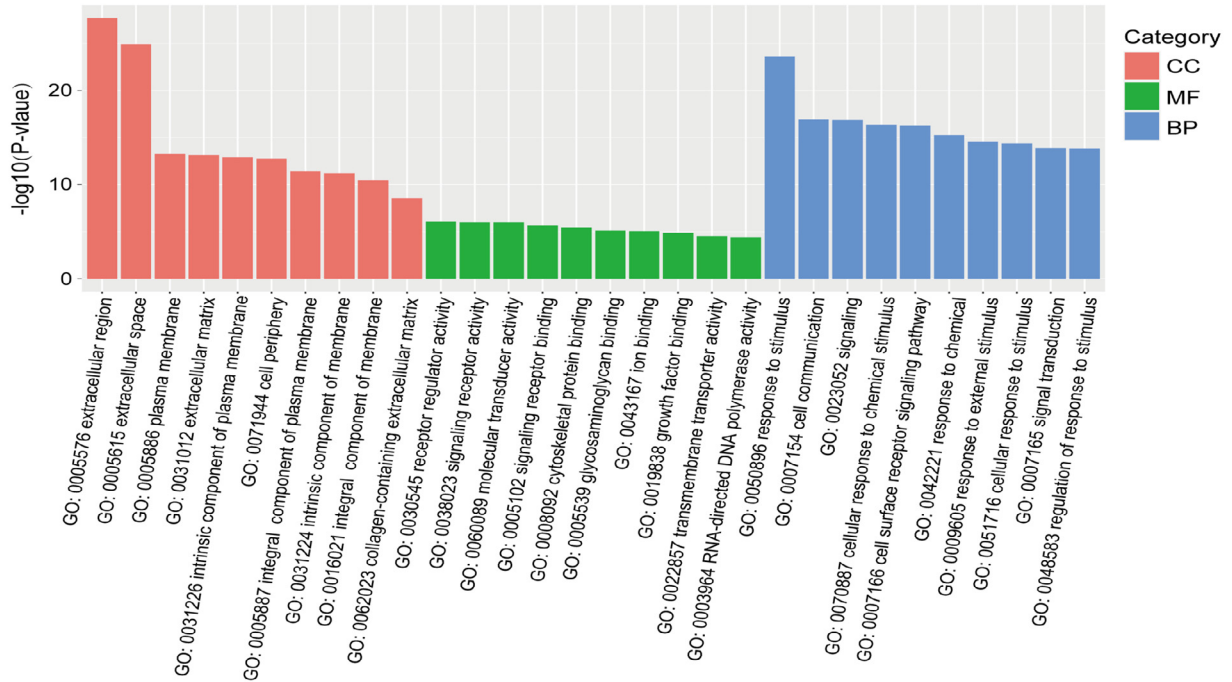
The reference genome of Ensembl of sequencing unigenes was assessed and annotated NCBI and 5 additional

databases. Among these, 16,779 unigenes underwent annotation from the 6 cDNA libraries. In the aforementioned database, the annotation numbers and percentages of genes are shown in Figure 1C.

### DGE Analysis

Of the 16,779 unigenes, 2,762 DEGs from GCs of ovarian follicles (6 to 8-mm diameter; SYF) were determined in the 6 cDNA libraries, with 1,605 significantly upregulated and 1,157 markedly downregulated unigenes ( $|\log_2\text{FoldChange}| > 1$ ,  $P < 0.05$ ;

A



B

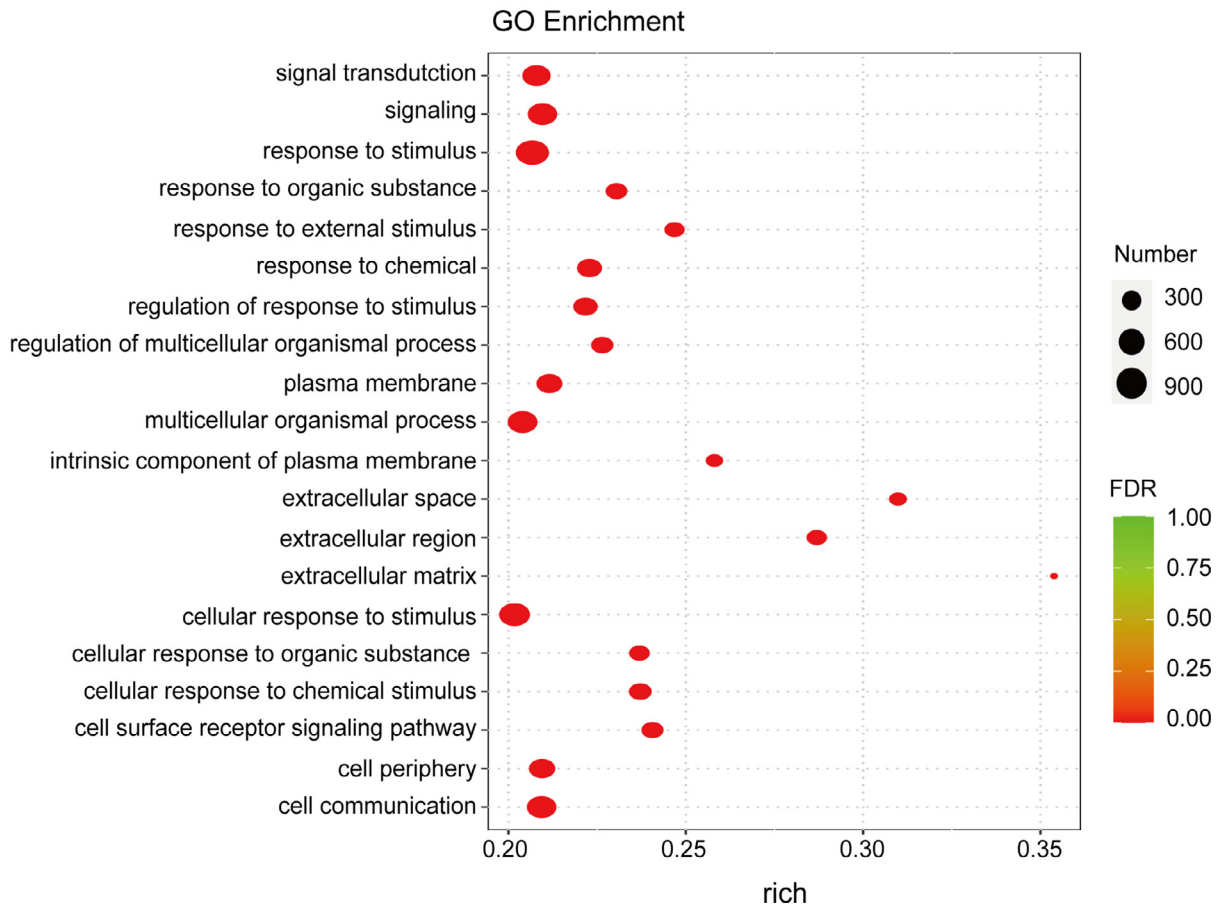
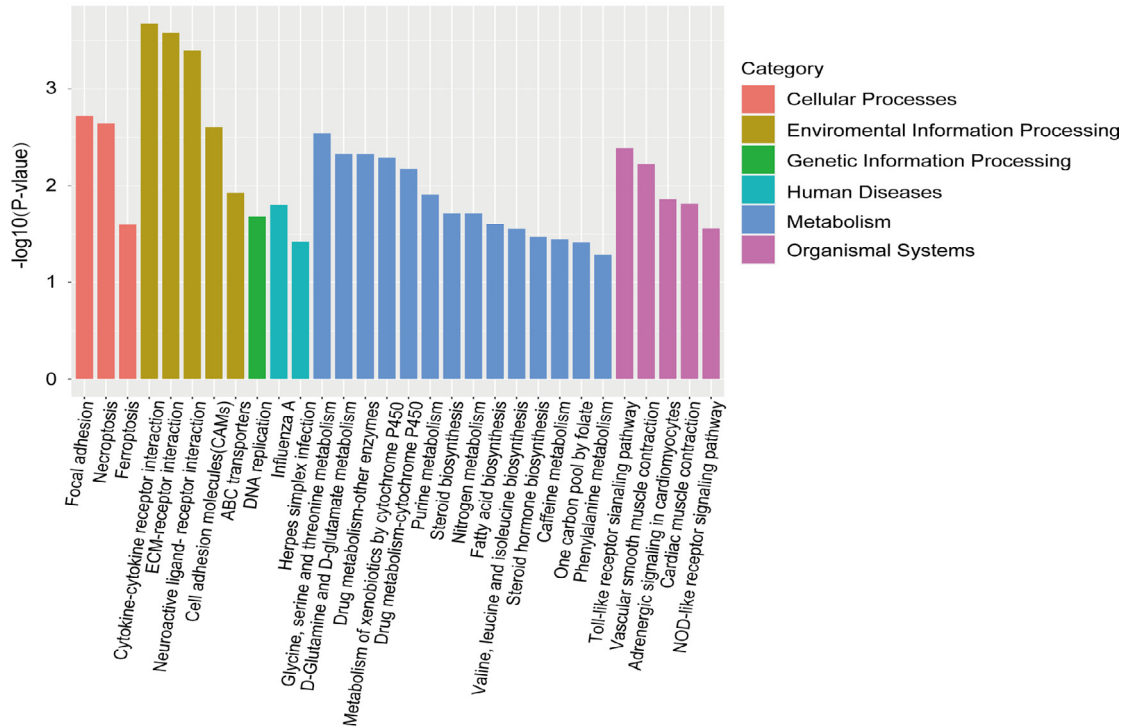


**Figure 3.** GO enrichment analysis of DEGs between *csal1* overexpressing and nontransfected granulosa cells from hen ovarian prehierarchal follicles. (A) The bar plot of Go enrichment analysis. X-axis, GO terms: biological process, cellular component, and molecular function. Y-axis,  $-\log_{10}(P\text{-value})$  of each term. (B) Bubble diagram of GO enrichment analysis. Circles of different sizes represent quantities, and different colors represent distinct FDR values.

A



B

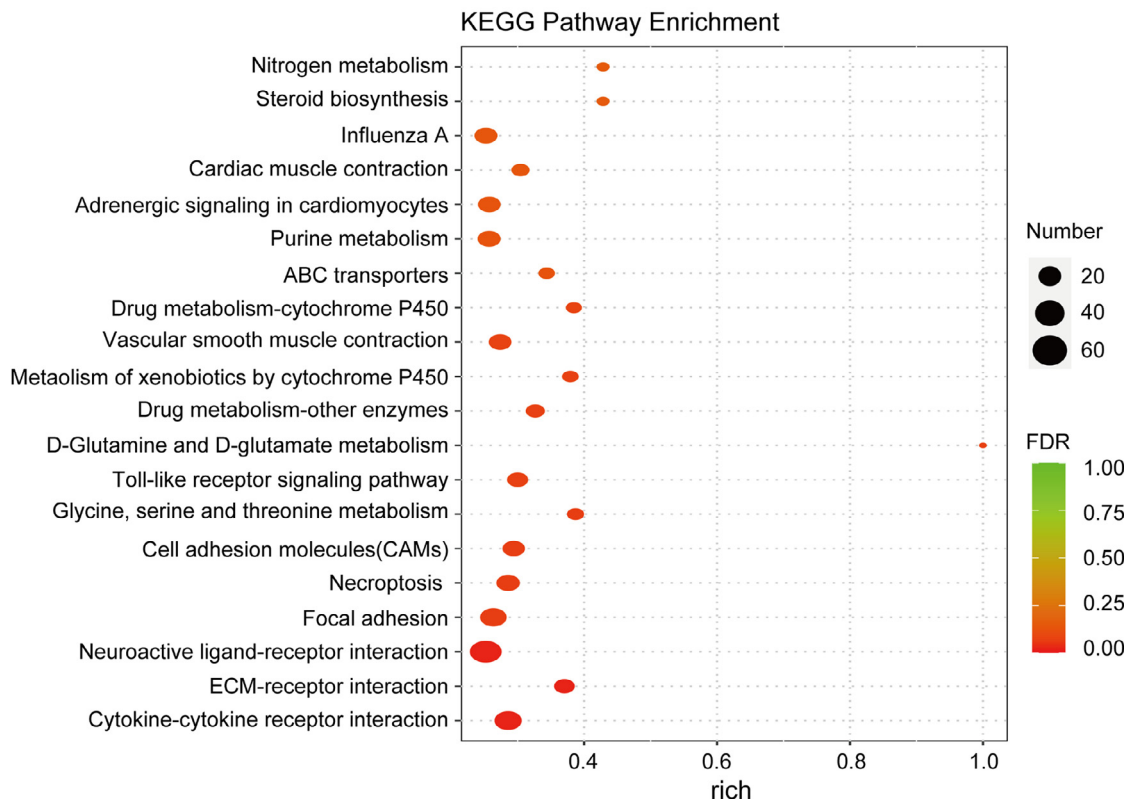


**Figure 4.** KEGG pathway enrichment analysis of DEGs between *csal1* overexpressing and non-transfected granulosa cells from hen ovarian pre-hierarchical follicles. (A) The bar plot of KEGG pathway enrichment analysis. X-axis, GO terms: cellular processes, environmental information processing, genetic information processing, human diseases, metabolism, organismal systems. Y-axis,  $-\log_{10}(P\text{-value})$  of every term. (B) Bubble diagram of KEGG pathway enrichment analysis. Circles of different sizes represent quantities, and different colors represent distinct FDR values.

Figures 2A and 2B). The FPKM hierarchical clustering map (Figure 2C) visually represents gene expression patterns in the specimens and highlighted data repeatability and accuracy.

### GO Analysis of DEGs

Based on the comparison of GCs from ovarian PFs in the *csal1* overexpression and control groups, 2,762

**Table 2.** List of partially representative DEGs.

Genes	Different expression type	Description	log2FoldChange	pval	KEGG	UniProtAC	eggNOG
BMP5	Upregulated	bone morphogenetic protein 5	2.207191257	2.84E-17	K04663	P87373	veNOG00413
TACR2	Upregulated	tachykinin receptor 2	2.592664911	0.027384	K04223	-	veNOG07359
AMH	Upregulated	anti-Mullerian hormone	5.012564505	6.5E-206	K04665	Q788U7	veNOG16048
PLAG1	Upregulated	PLAG1 zinc finger	1.273295028	6.69E-09	K19484	Q58NQ5	veNOG02243
MYOD1	Downregulated	myogenic differentiation 1	-2.084990972	0.006683	K09064	P16075	opiNOG36948; veNOG00749
BOP1	Downregulated	block of proliferation 1	-1.992773591	1.14E-27	-	-	veNOG15316;fiNOG04039
SIPA1	Downregulated	signal-induced proliferation-associated 1-like protein 3-like	-1.242977568	0.000297	-	-	veNOG04528
NOTCH1	Downregulated	notch 1	-1.77078885	1.46E-24	K02599	F1NZ70	veNOG02575
BCL2L1	Downregulated	BCL2 like 1	-1.458977008	2.23E-10	K04570	Q07816	veNOG10445
SOX9	Downregulated	SRY (sex determining region Y)-box 9	-1.722821315	1.12E-12	K18435	P48434	veNOG11187
ADGRA2	Downregulated	adhesion G protein-coupled receptor A2	-1.045490949	8.4E-05	K08461	-	veNOG03321
WNT5A	Down-regulated	Wnt family member 5A	-2.532140807	0.000399	K00444	Q9YGX6	veNOG08444
SLC7A11	Downregulated	solute carrier family 7 member 11	-2.760443999	1.57E-28	K13869	-	veNOG05087
GATAD2B	Downregulated	GATA zinc finger domain containing 2B	-1.463635505	1.85E-16	-	-	veNOG13402

DEGs were enriched in 12,184 distinct GO terms. A total of 9,157, 1,013, and 2,014 DEGs were assigned to the BP, CC, and MF GO categories, respectively. The top 10 GO terms with significance for BP, CC and MF are shown in [Figure 3A](#) ( $P < 0.05$ ). This finding also indicated that the main function of *csal1* involved biological processes in ovarian follicle development. Based on GO enrichment data, enrichment degree was assessed by the richness factor, FDR and the amounts of genes enriched in a given GO term. The higher the richness factor, the higher the degree of enrichment, the more significant the enrichment. The top 20 GO terms with the lowest FDRs are displayed in [Figure 3B](#). Moreover, the top 10 GO terms for BP, MF, and CC are shown in the GO DAG structure (Supplementary Figure 2).

### KEGG Pathways Involving the DEGs

KEGG pathway enrichment analysis was carried out to assess *csal1* overexpressing and nontransfected GCs from ovarian follicles of 6 to 8-mm diameter (SYF) to further reveal the most relevant signaling pathways associated with ovarian follicle development and identify GO-annotated DEGs involved in the transducing events. Among these, 30 most relevant pathways with remarkable enrichment are shown in [Figure 4A](#). To summarize, 534 DEGs from these 20 significantly KEGG pathways, including 342 upregulated and 192 downregulated, were enriched ([Figure 4B](#)).

### Transcription Factor Family Analysis

The transcription factors and their respective families were predicted and obtained through the comparison with the animal transcription factor database. About 2,073 transcription factors, which belonged to 69

transcription factor families, were obtained ([Figure 5](#)). The transcription factor family with the largest number of members was zf-C2H2, successively followed by homeobox and bHLH. They all had more than 200 members, and zf-C2H2 had 316 members.

### Protein Interaction Network

The associations among the protein products of the identified DEGs were analyzed for further clarifying the potential genetic mechanism of ovarian follicle development in chickens. The parameters were set to score  $>0.95$ . The protein-protein interaction network is depicted in [Figure 6](#). In PFs, interactions among 253 proteins were found. PLK1, TTK, CDC20, CENPC, INCENP, KIF4B, MCM, NCAPG, FGF, FN1, ORC1, RAC2, and VEGFC, which are mainly involved in mitosis, embryonic development and cell proliferation and differentiation, might be in central effectors for these interactions.

### Validation of the Selected DGEs by RT-qPCR

Fourteen candidate DGEs were chosen for RT-qPCR validation ([Table 2](#)), including 4 relevant upregulated genes (*BMP5*, *TACR2*, *AMH*, and *PLAG1*) and 10 related downregulated genes (*MYOD1*, *BOP1*, *SIPA1*, *NOTCH1*, *BCL2L1*, *SOX9*, *ADGRA2*, *WNT5A*, *SLC7A11*, and *GATAD2B*). As shown in [Figure 7](#), all 4 DGEs upregulated in RNA-seq were upregulated in GCs with *csal1* overexpression from ovarian PFs. The 10 tested downregulated DGEs were also downregulated. These results showed that differences in the expression levels of these candidate DGEs detected by RT-qPCR were consistent with RNA-seq data. The observed



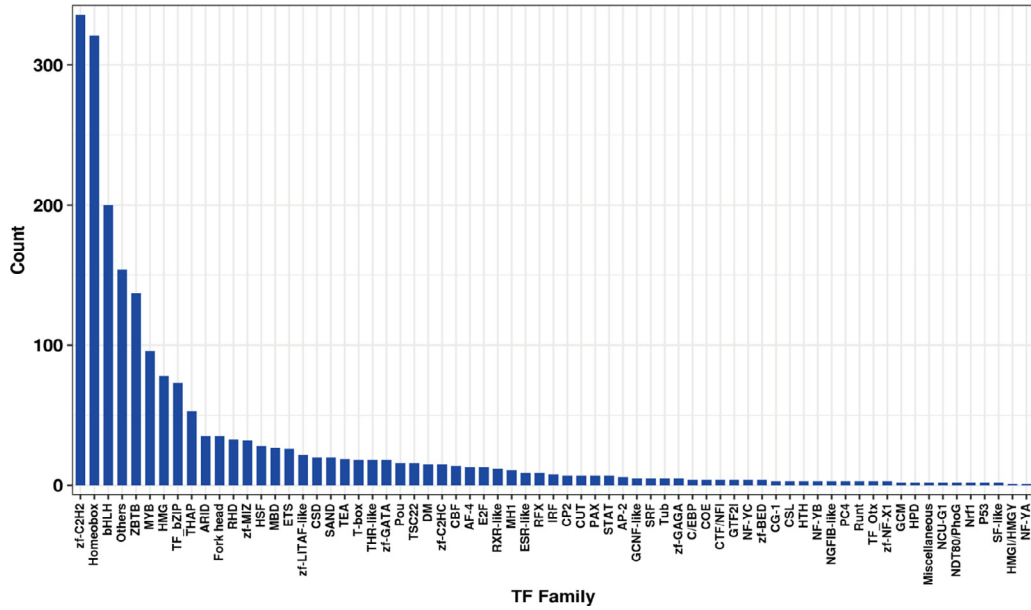


**Figure 5.** Statistical map of transcription factor family. X-axis, different transcription factor families. Y-axis, number of genes falling into a given transcription factor family.

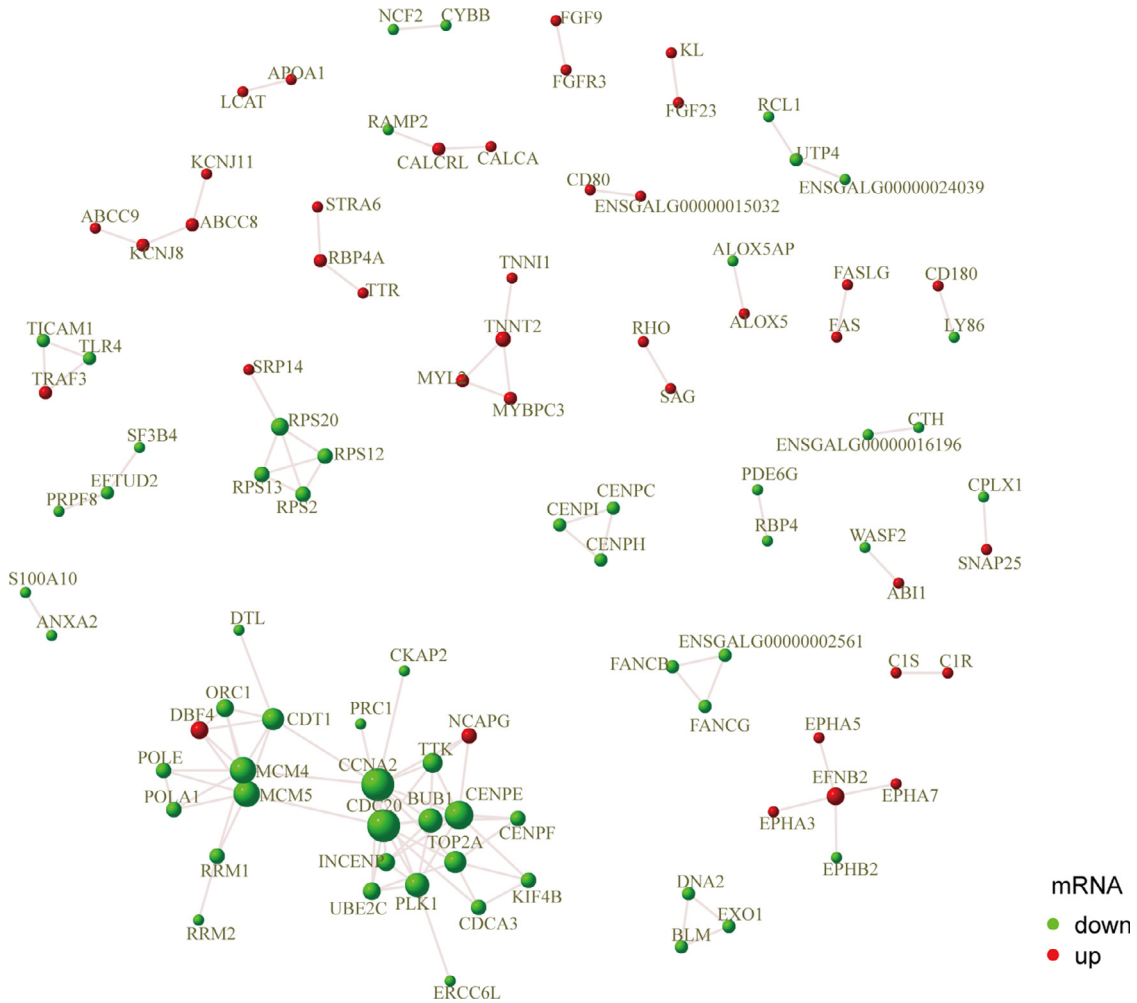


**Figure 6.** Predicted protein-protein interaction network. The points in the figure are genes (corresponding proteins). Red and green indicate upregulated and downregulated genes, respectively.

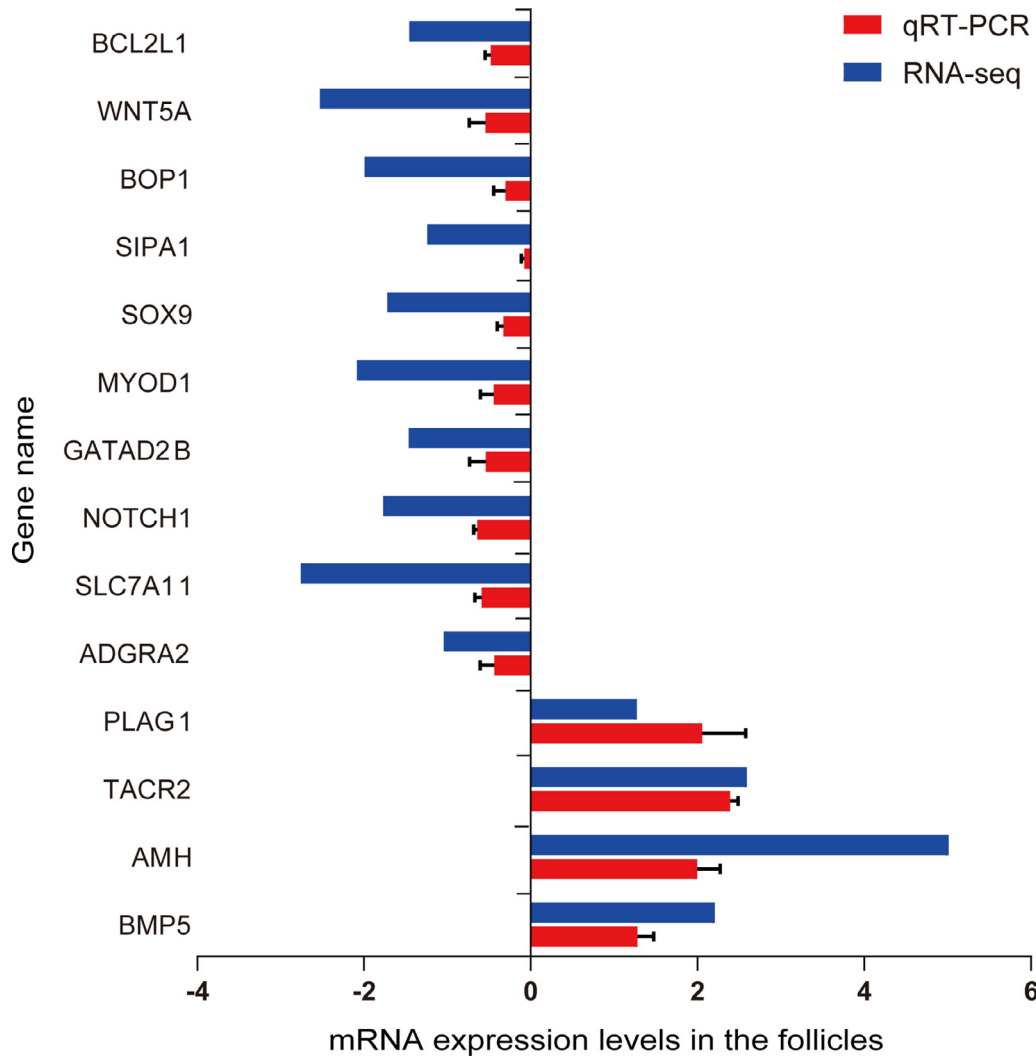


**Figure 7.** Gene expression levels (Log<sub>2</sub>FC) of 14 candidate genes assessed by RNA-Seq and RT-qPCR. Relative expression levels for various genes were obtained by the  $2^{-\Delta\Delta C_t}$  method with 18S rRNA as a reference gene.

expression trends confirmed the RNA-seq results, implying that the above RNA-seq results were reliable.

## DISCUSSION

The egg production trait, which is a critical feature in the global poultry industry, is affected by follicular development. Follicles at distinct developmental stages have different molecular features and functions in ovary growth and development. In particular, the genetic regulation of 6 to 8-mm diameter follicles contributes to follicle selection (Johnson and Woods, 2009; Johnson, 2015) and may have a unique effect on the hierarchy of undifferentiated PFs. Therefore, SYF (6 to 8-mm diameter) was selected in this study. Multiple reports identified factors controlling follicular development and the selection of undifferentiated PFs into the differentiated pre-ovulatory follicle hierarchy (Johnson, 2015; Xu et al., 2018). Among these, our previous study revealed that *csal1* suppresses the GC proliferation and steroidogenesis (Zhu et al., 2019). However, the exact regulatory effect of *csal1* in PF development remains undefined.

The high-throughput sequencing technology, for example, RNA-seq, has been widely used in animal breeding research. RNA-Seq could assess the expression levels, structures, and modulatory profiles of genes by examining the transcriptomes of different cells or tissues. The recent findings provide novel insights into reproduction in chickens and identify effective biomarkers for genetic improvement in the chicken breed (Wang and Ma, 2019; Zhang et al., 2019; Mishra et al., 2020; Chen, et al., 2021).

Here, transcriptome analysis indicated that the main function of *csal1* is to regulate BP in ovarian follicle development. Of which, 14 DEGs were screened, which were related to GC proliferation, differentiation, hormone production, ovarian follicular development, regulation of reproductive processes, and signaling pathways in the PFs of hen ovary included *BMP5*, *TACR2*, *AMH*, *PLAG1*, *MYOD1*, *BOP1*, *SIPA1*, *NOTCH1*, *BCL2L1*, *SOX9*, *ADGRA2*, *WNT5A*, *SLC7A11*, and *GATAD2B*. In addition, the 14 DEGs were characterized by KEGG pathway enrichment analysis, 14 DEGs were enriched in 13 KEGG pathways, including cytokine–cytokine receptor interaction, neuroactive ligand–receptor

interaction, progesterone-mediated oocyte maturation, Wnt signaling pathway, and TGF- $\beta$  signaling pathway, which were significantly enriched and are involved in signaling molecules and interaction, endocrine system, amino acid biosynthesis and metabolism, signal transduction, and cell growth and death. The identified DEGs were tightly associated with multiple physiological events of follicle growth and development, indicating their possible involvement in hen egg-laying potential.

The DEGs identified in this study included many receptor genes, such as follicle-stimulating hormone receptor (**FSHR**), estrogen receptor 1 (**ESR1**), nerve growth factor receptor (**NGFR**), G protein-coupled receptor (**GPCR**), gamma-aminobutyric acid type A receptor (**GABRP**), interleukin-1 receptor (**IL1RL1**), and so on. Of these genes, follicle-stimulating hormone (**FSH**) represents a key player in germ cell formation (Wang et al., 2021b). It participates in GC proliferation, antrum formation in secondary ovarian follicles, antral follicle development and estradiol biosynthesis, ultimately promoting folliculogenesis, oogenesis, oocyte meiotic maturation, and oocyte competence (Padmanabhan and Cardoso, 2020). FSH secretion relies on the HPG axis. FSH represents a glycoprotein with  $\alpha$  and  $\beta$  subunits bound by non-covalent interactions (Das and Kumar, 2018). FSH $\beta$  affects target cells (GCs) when connected to its FSHR in the cell membrane (Szymańska et al., 2018). FSHR is a member of the G protein-coupled receptor (**GPCR**) family, which activates diverse pathways such as cAMP/PKA, PKC/MAPK and Ca<sup>+</sup>/CaMKII pathways (Szymańska et al., 2018). In addition, recent findings showed that FSH has new functions, such as regulation of bone formation, fat metabolism, energy homeostasis, cholesterol biosynthesis, and cardiovascular pathologies by interacting with its receptor, FSHR (Recchia et al., 2021).

Anti-Mullerian hormone (**AMH**) is secreted by the GCs of primary and preantral follicles, affecting folliculogenesis mainly by suppressing preantral follicles' sensitivity to FSH and downregulating aromatase, inducing dominant follicle selection. In addition, AMH suppresses the growth of primordial follicles in the ovarian reserve, thereby suppressing follicular development (Dewailly et al., 2016). The AMH effect was further demonstrated by FSH treatment of pre-pubertal AMH (-/-) mice, promoting follicle growth. Similar findings have been obtained in a human study examining AMH added to culture GCs (Durlinger et al., 2001; Pellatt et al., 2011). AMH amounts are elevated during puberty because of the elevated oocyte maturation rate, and low in menopause, which was consistent with this study. Not only their systemic regulation by hormones (gonadotropins) but also their intraovarian regulation by gonadal steroids, growth factors, cytokines, and intracellular proteins, such as B cell lymphoma/leukemia 2 (**BCL2**) family members which are widely expressed in embryonic tissues (Matsuda et al., 2012). As one of the key transcription factors governing early gonad's differentiation, SOX9 was abnormally expressed in exposed ovary, while the formation of follicle was

partially restored by SOX9 knockdown (Qiqi et al., 2022). The expression of Sox9 is regulated by members of the FGF, transforming growth factor-b (**TGF-b**), Wnt families, and bone morphogenetic protein (**BMP**) (Quintana et al., 2009). And BMP-SMAD1/5/8 signaling is critical for follicular activation and development, as well as GC proliferation, atresia and luteinization. In addition, Notch signaling is also induced by gonadotrophins, with a critical role in oocyte development (Jozkowiak et al., 2020).

Among the DEGs, solute carrier family 7 member 11 (**SLC7A11**) was significantly downregulated after the overexpression of *csal1*. Although the physiological function of the SLC7A family has been widely explored in mammals, such studies are scarce in poultry. SLC7A11 (or xCT), a cystine and glutamate antiporter, imports cystine for glutathione synthesis and antioxidation (Xu et al., 2021). The SLC7A family comprises sodium-independent amino acid transporters inducing the transport of multiple amino acids, including glycine, serine, alanine and cysteine. As neuronal transporters, they primarily regulate excitatory glutamatergic neurotransmission (Sawada et al., 2002). Amino acids regulate the reproductive, cardiovascular, and immune systems, implying their metabolism in the pituitary gland may be critical in modulating reproduction in chickens. Therefore, we speculated SLC7A11 downregulation after *csal1* overexpression controlling amino acid synthetic, transport, and metabolic pathways might result in altered amino acid use, which might influence the development and functions of downstream target organs via the endocrine vasculature, finally affecting reproductive physiology and egg-laying potential in hens.

The spalt members, featuring many C2H2-type zinc finger (**ZF**) motifs, are transregulators of genes in growth and developmental events. Of these, SALL1 can interact with  $\beta$ -catenin and synergistically activate a reporter construct that responds to Wnt signaling by recruiting remodeling factors to heterochromatin (Zhu et al., 2019). In this study, DEGs related to the ZF structure and Wnt/ $\beta$ -catenin signaling pathway were also screened, such as ovo like ZF 2 (**OVOL2**) and pleomorphic adenoma gene 1 (**PLAG1**), Wnt family member 5A (**Wnt5A**), Dickkopf Wnt signaling pathway inhibitor 3 (Liu et al., 2021), and frizzled related protein (Tuerlings et al., 2022).

Previous studies reported PLAG1 encodes a ZF transcription factor. PLAG1 contributes to HGMA2-PLAG1-IGF2 signaling that after disruption causes Silver-Russell syndrome, which is manifested by severe intrauterine growth restriction. PLAG1 is abundant during development in the mouse brain (Tran et al., 2021). It constitutes cell proliferation via direct regulation of multiple target genes, for example, many growth factors, including IGF2 (Van Dyck et al., 2007). Also, PLAG1-deficient mice show growth retardation, which is presumed to be associated with IGF2 regulation by PLAG1 to some extent (Hensen et al., 2004). Further, it was shown PLAG1 controls milk production, reproductive potential, muscle generation, and body height in

livestock (Fink et al., 2017). This suggested that PLAG1 affects growth and embryonic development in domesticated animals, possibly in follicles, which corroborated our results. As one of the subunits forming the nucleosome remodeling and histone deacetylation complex, GATA ZF domain containing 2B (**GATAD2B**) is critical in chromatin alteration and transcriptional modulation (Wang et al., 2021a). This structure and function are highly consistent with those of *csal1*. Wnt5A represents a Wnt family member transcriptionally regulated by Wnt signaling, greatly affecting cell proliferation, differentiation, migration and movement. Wnt5A also contributes to development, homeostasis and disease (Astudillo, 2022). The growth of hair follicles is controlled by diverse pathways, for example, Wnt, Bmp, Notch, and others. Of these, Wnt signaling is critically important. In addition, overexpressed Wnt5a promotes  $\beta$ -catenin degradation, inhibits the classical Wnt/ $\beta$ -catenin pathway and suppresses hair follicle growth (Wei et al., 2022). Generally speaking, these results corroborated the aforementioned findings.

Here, the screened DEGs contributed to controlling GC proliferation, differentiation and apoptosis, oocyte meiosis and maturation, follicular differentiation and atresia, and gonadotrophin-release hormone secretion through crosstalk or interactions with multiple pathways. These findings provide compelling evidence of the significant differences in gene expression levels in the whole genome during the follicular development in Chinese Dagu chickens, which confirmed the role of *csal1* in follicular development. Taken together, the present data provide new insights into the regulation of follicular development in chickens.

## CONCLUSIONS

In summary, this study was the first to reveal the transcriptome analysis of GCs from ovarian PFs (SYF) between those with overexpression of *csal1* and normal ones. The current data suggested that the screened DGEs could constitute a basis for in-depth exploration of the mechanism by which *csal1* controls genes that contribute to PF development and growth in the hen ovary from Chinese Dagu chickens in vivo. This study also explored the biological events and pathways associated with egg-laying and follicle development in chickens. An ongoing study by our team aims to precisely examine the regulatory role of the *csal1* gene in PF development, which could provide major insights into the methods for improving egg production in poultry. Finally, identifying valuable biomarkers of the egg-laying trait could improve breeding programs to enhance egg production by Chinese Dagu chickens.

## ACKNOWLEDGMENTS

This work was supported by the National Natural Science Foundation of China [grant number 32002154]; the Natural Science Foundation of Liaoning Province [grant

number 2021-BS-262]; Basic scientific research projects of Liaoning Education Department [grant number LJKMZ20221240]; and the Training Programs of Innovation and Entrepreneurship for Undergraduates of Jinzhou Medical University [grant number 201824]

## DISCLOSURES

The authors declare no conflicts of interest.

## SUPPLEMENTARY MATERIALS

Supplementary material associated with this article can be found in the online version at [doi:10.1016/j.psj.2022.102310](https://doi.org/10.1016/j.psj.2022.102310).

## REFERENCES

- Ashburner, M., C. A. Ball, J. A. Blake, D. Botstein, H. Butler, J. M. Cherry, A. P. Davis, K. Dolinski, S. S. Dwight, J. T. Eppig, M. A. Harris, D. P. Hill, L. Issel-Tarver, A. Kasarskis, S. Lewis, J. C. Matese, J. E. Richardson, M. Ringwald, G. M. Rubin, and G. Sherlock. 2000. Gene ontology: tool for the unification of biology. *The Gene Ontology Consortium. Nat. Genet.* 25:25–29.
- Astudillo, P. 2022. An emergent Wnt5a/YAP/TAZ regulatory circuit and its possible role in cancer. *Semin. Cell Dev. Biol.* 125:45–54.
- Chen, X., X. Sun, I. M. Chimbaka, N. Qin, X. Xu, S. Liswaniso, R. Xu, and J. M. Gonzalez. 2021. Transcriptome analysis of ovarian follicles reveals potential pivotal genes associated with increased and decreased rates of chicken egg production. *Front. Genet.* 12:622751.
- Das, N., and T. R. Kumar. 2018. Molecular regulation of follicle-stimulating hormone synthesis, secretion and action. *J. Mol. Endocrinol.* 60:R131–R155.
- Dewailly, D., G. Robin, M. Peigne, C. Decanter, P. Pigny, and S. Catteau-Jonard. 2016. Interactions between androgens, FSH, anti-Mullerian hormone and estradiol during folliculogenesis in the human normal and polycystic ovary. *Hum. Reprod. Update* 22:709–724.
- Durlinger, A. L., M. J. Gruijters, P. Kramer, B. Karels, T. R. Kumar, M. M. Matzuk, U. M. Rose, F. H. de Jong, J. T. Uilenbroek, J. A. Grootegoed, and A. P. Themmen. 2001. Anti-Mullerian hormone attenuates the effects of FSH on follicle development in the mouse ovary. *Endocrinology* 142:4891–4899.
- Fink, T., K. Tiplady, T. Lopdell, T. Johnson, R. G. Snell, R. J. Spellman, S. R. Davis, and M. D. Littlejohn. 2017. Functional confirmation of PLAG1 as the candidate causative gene underlying major pleiotropic effects on body weight and milk characteristics. *Sci. Rep.* 7:44793.
- Gilbert, A. B., M. M. Perry, D. Waddington, and M. A. Hardie. 1983. Role of atresia in establishing the follicular hierarchy in the ovary of the domestic hen (*Gallus domesticus*). *J. Reprod. Fertil.* 69:221–227.
- Hensen, K., C. Braem, J. Declercq, F. Van Dyck, M. Dewerchin, L. Fiette, C. Denef, and W. J. Van de Ven. 2004. Targeted disruption of the murine *Plag1* proto-oncogene causes growth retardation and reduced fertility. *Dev. Growth Differ.* 46:459–470.
- Johnson, A. L. 2015. Ovarian follicle selection and granulosa cell differentiation. *Poult. Sci.* 94:781–785.
- Johnson, A. L., and D. C. Woods. 2009. Dynamics of avian ovarian follicle development: cellular mechanisms of granulosa cell differentiation. *Gen. Comp. Endocrinol.* 163:12–17.
- Jozkowiak, M., G. Hutchings, M. Jankowski, K. Kulcenty, P. Mozdziak, B. Kempisty, R. Z. Spaczynski, and H. Piotrowska-Kempisty. 2020. The stemness of human ovarian granulosa cells and the role of resveratrol in the differentiation of MSCs—a review based on cellular and molecular knowledge. *Cells* 9:1418.
- Kim, D., J. M. Paggi, C. Park, C. Bennett, and S. L. Salzberg. 2019. Graph-based genome alignment and genotyping with HISAT2 and HISAT-genotype. *Nat. Biotechnol.* 37:907–915.

- Liu, W., L. Ma, and J. Zhang. 2021. MicroRNA-934 promotes colorectal cancer cell proliferation by directly targeting Dickkopf-related protein 2. *Exp. Ther. Med.* 22:1041.
- Lyu, Z., N. Qin, T. L. Tyasi, H. Zhu, D. Liu, S. Yuan, and R. Xu. 2016. The Hippo/MST pathway member SAV1 plays a suppressive role in development of the prehierarchal follicles in hen ovary. *PLoS One* 11:e0160896.
- Matsuda, F., N. Inoue, N. Manabe, and S. Ohkura. 2012. Follicular growth and atresia in mammalian ovaries: regulation by survival and death of granulosa cells. *J. Reprod. Dev* 58:44–50.
- Miao, X., Q. Luo, and X. Qin. 2016. Genome-wide transcriptome analysis in the ovaries of two goats identifies differentially expressed genes related to fecundity. *Gene* 582:69–76.
- Mishra, S. K., B. Chen, Q. Zhu, Z. Xu, C. Ning, H. Yin, Y. Wang, X. Zhao, X. Fan, M. Yang, D. Yang, Q. Ni, Y. Li, M. Zhang, and D. Li. 2020. Transcriptome analysis reveals differentially expressed genes associated with high rates of egg production in chicken hypothalamic-pituitary-ovarian axis. *Sci. Rep.* 10:5976.
- Nelson, L. R., and S. E. Bulun. 2001. Estrogen production and action. *J. Am. Acad. Dermatol.* 45:S116–S124.
- Padmanabhan, V., and R. C. Cardoso. 2020. Neuroendocrine, autocrine, and paracrine control of follicle-stimulating hormone secretion. *Mol. Cell Endocrinol.* 500:110632.
- Pellatt, L., S. Rice, N. Dilaver, A. Heshri, R. Galea, M. Brincat, K. Brown, E. R. Simpson, and H. D. Mason. 2011. Anti-Mullerian hormone reduces follicle sensitivity to follicle-stimulating hormone in human granulosa cells. *Fertil. Steril.* 96 1246–51e1.
- Perlea, M., D. Kim, G. M. Perlea, J. T. Leek, and S. L. Salzberg. 2016. Transcript-level expression analysis of RNA-seq experiments with HISAT, StringTie and Ballgown. *Nat. Protoc.* 11:1650–1667.
- Qiqi, L., H. Junlin, C. Xuemei, H. Yi, L. Fangfang, G. Yanqing, Z. Yan, J. Lamptey, C. Zhuxiu, L. Fangfei, W. Yingxiang, and M. Xinyi. 2022. Fetal exposure of Aristolochic Acid I undermines ovarian reserve by disturbing primordial folliculogenesis. *Ecotoxicol. Environ. Saf.* 236:113480.
- Quintana, L., N. I. zur Nieden, and C. E. Semino. 2009. Morphogenetic and regulatory mechanisms during developmental chondrogenesis: new paradigms for cartilage tissue engineering. *Tissue Eng. Part B Rev.* 15:29–41.
- Recchia, K., A. S. Jorge, L. V. F. Pessoa, R. C. Botigelli, V. C. Zugaib, A. F. de Souza, D. D. S. Martins, C. E. Ambrosio, F. F. Bressan, and N. C. G. Pieri. 2021. Actions and roles of FSH in germinative cells. *Int. J. Mol. Sci.* 22:10110.
- Sawada, H., Y. Takahashi, J. Fujino, S. Y. Flores, and H. Yokosawa. 2002. Localization and roles in fertilization of sperm proteasomes in the ascidian *Halocynthia roretzi*. *Mol. Reprod. Dev.* 62:271–276.
- Sweetman, D., T. G. Smith, E. R. Farrell, and A. Munsterberg. 2005. Expression of *csal1* in pre limb-bud chick embryos. *Int. J. Dev. Biol.* 49:427–430.
- Szymanska, K., J. Kalafut, A. Przybyszewska, B. Paziewska, G. Adamczuk, M. Kielbus, and A. Rivero-Muller. 2018. FSHR transactivation and oligomerization. *Front. Endocrinol (Lausanne)* 9:760.
- Tran, S. C., E. J. Jaehne, L. E. Dye, J. Wong, J. S. Bakas, J. G. Gasperoni, M. W. Hale, M. van den Buuse, S. Dworkin, S. V. H. Grommen, and B. De Groef. 2021. Effect of pleomorphic adenoma gene 1 deficiency on selected behaviours in adult mice. *Neuroscience* 455:30–38.
- Tuerlings, M., M. van Hoolwerff, J. M. van Bokkum, H. E. D. Suchiman, N. Lakenberg, D. Broekhuis, R. Nelissen, Y. F. M. Ramos, H. Mei, D. Cats, R. Coutinho de Almeida, and I. Meulenbelt. 2022. Long non-coding RNA expression profiling of subchondral bone reveals AC005165.1 modifying FRZB expression during osteoarthritis. *Rheumatology (Oxford)* 61:3023–3032.
- Van Dyck, F., J. Declercq, C. V. Braem, and W. J. Van de Ven. 2007. PLAG1, the prototype of the PLAG gene family: versatility in tumour development (review). *Int. J. Oncol.* 30:765–774.
- Wang, B., S. Zhu, Y. Deng, X. Sai, Z. Chen, J. Liu, G. Li, N. Liu, J. Chen, C. Yu, T. Sun, and P. Zhu. 2021a. Establishment of a CRISPR/Cas9-mediated GATAD2B homozygous knockout human embryonic stem cell line. *Stem Cell Res.* 57:102590.
- Wang, C., and W. Ma. 2019. Hypothalamic and pituitary transcriptome profiling using RNA-sequencing in high-yielding and low-yielding laying hens. *Sci. Rep.* 9:10285.
- Wang, H. Q., W. D. Zhang, B. Yuan, and J. B. Zhang. 2021b. Advances in the regulation of mammalian follicle-stimulating hormone secretion. *Animals (Basel)* 11:1134.
- Wang, L., Z. Feng, X. Wang, X. Wang, and X. Zhang. 2010. DEGseq: an R package for identifying differentially expressed genes from RNA-seq data. *Bioinformatics* 26:136–138.
- Wei, H., X. Xu, S. Yang, C. Liu, Q. Li, and P. Jin. 2022. The potential role of *hsa\_circ\_0001079* in androgenetic alopecia via sponging *hsa-miR-136-5p*. *J. Clin. Lab. Anal.* 36:e24021.
- Woodruff, T. K., and L. D. Shea. 2007. The role of the extracellular matrix in ovarian follicle development. *Reprod. Sci.* 14:6–10.
- Wu, Y., X. Zhao, L. Chen, J. Wang, Y. Duan, H. Li, and L. Lu. 2020. Transcriptomic analyses of the hypothalamic-pituitary-gonadal axis identify candidate genes related to egg production in Xinjiang Yili Geese. *Animals (Basel)* 10:90.
- Xu, F., Y. Guan, L. Xue, P. Zhang, M. Li, M. Gao, and T. Chong. 2021. The roles of ferroptosis regulatory gene *SLC7A11* in renal cell carcinoma: a multi-omics study. *Cancer Med.* 10:9078–9096.
- Xu, R., N. Qin, X. Xu, X. Sun, X. Chen, and J. Zhao. 2018. Inhibitory effect of *SLIT2* on granulosa cell proliferation mediated by the *CDC42-PAKs-ERK1/2* MAPK pathway in the prehierarchal follicles of the chicken ovary. *Sci. Rep* 8:9168.
- Yang, K. T., C. Y. Lin, H. L. Huang, J. S. Liou, C. Y. Chien, C. P. Wu, C. W. Huang, B. R. Ou, C. F. Chen, Y. P. Lee, E. C. Lin, P. C. Tang, W. C. Lee, S. T. Ding, W. T. Cheng, and M. C. Huang. 2008. Expressed transcripts associated with high rates of egg production in chicken ovarian follicles. *Mol. Cell. Probes.* 22:47–54.
- Zhang, T., L. Chen, K. Han, X. Zhang, G. Zhang, G. Dai, J. Wang, and K. Xie. 2019. Transcriptome analysis of ovary in relatively greater and lesser egg producing Jinghai Yellow Chicken. *Anim. Reprod. Sci.* 208:106114.
- Zhu, H., N. Qin, T. L. Tyasi, Y. Jing, D. Liu, S. Yuan, and R. Xu. 2018. Genetic effects of the transcription factors-sal-like 1 and spalt-like transcription factor 3 on egg production-related traits in Chinese Dagu hens. *J. Exp. Zool. A Ecol. Integr. Physiol.* 329:23–28.
- Zhu, H., N. Qin, X. Xu, X. Sun, X. Chen, J. Zhao, R. Xu, and B. Mishra. 2019. Synergistic inhibition of *csal1* and *csal3* in granulosa cell proliferation and steroidogenesis of hen ovarian prehierarchal developmentdagger. *Biol. Reprod.* 101:986–1000.